Geomechanics and Engineering, *Vol. 8, No. 6 (2015) 769-781*
DOI: http://dx.doi.org/10.12989/gae.2015.8.6.769

An analytical analysis of a single axially-loaded pile using a nonlinear softening model

Yue-dong Wu [1,2a], Jian Liu [1,2b] and Rui Chen [*3]

[1] *Key Laboratory of Ministry of Education for Geomechanics and Embankment Engineering, Hohai University, Nanjing 210098, China*
[2] *Geotechnical Research Institute, Hohai University, Nanjing 210098, China*
[3] *Shenzhen Key Laboratory of Urban and Civil Engineering for Disaster Prevention and Mitigation, Shenzhen Graduate School, Harbin Institute of Technology, Shenzhen University Town, Xili, Shenzhen, China*

(*Received October 06, 2014, Revised January 24, 2015, Accepted January 31, 2015*)

Abstract. The skin friction of a pile foundation is important and essential for its design and analysis. More attention has been given to the softening behaviour of skin friction of a pile. In this study, to investigate the load-transfer mechanism in such a case, an analytical solution using a nonlinear softening model was derived. Subsequently, a load test on the pile was performed to verify the newly developed analytical solution. The comparison between the analytical solution and test results showed a good agreement in terms of the axial force of the pile and the stress-strain relationship of the pile-soil interface. The softening behaviour of the skin friction can be simulated well when the pile is subjected to large loads; however, such behaviour is generally ignored by most existing analytical solutions. Finally, the effects of the initial shear modulus and the ratio of the residual skin friction to peak skin friction on the load-settlement curve of a pile were investigated by a parametric analysis.

Keywords: nonlinear softening model; single pile; land-transfer mechanism; skin friction; analytical analysis

1. Introduction

Pile foundations are required to support large loads from superstructures when shallow foundations are inadequate. The applied loads on a pile are counterbalanced by skin friction along the pile and the bearing resistance at the pile toe. The skin friction is mobilised when the pile moves downward relative to its surrounding soils, whereas the toe bearing is determined by the difference between the applied loads and the resistance from the skin friction. In other words, toe bearing is affected by the mobilization of skin friction (Madhav *et al*. 2009). Methods used to determine skin friction and toe bearing of a pile for engineering designs are mostly empirical and semi-theoretical. For example, empirical factors are used to estimate the resistance from skin friction (Poulos 1988). Regarding toe resistance, a coefficient (0.0372 for driven piles and 0.0465

*Corresponding author, Associate Professor, E-mail: chenrui1005@hotmail.com
[a] Associate Professor., E-mail: hhuwyd@163.com
[b] Ph.D. Student, E-mail: geoliujian@163.com

http://www.techno-press.org/?journal=gae&subpage=7 ISSN: 2005-307X (Print), 2092-6219 (Online)

for jacked piles) that was proposed by Vesic (1961) has been used to compute the resistance from the toe bearing and the settlement at the toe. Moreover, the Young's modulus, which is should be a material constant for a pile, is generally modified for design based on energy-corrected standard penetration tests (Mayne and Harris 1993). However, most empirical methods generally ignore the mechanism of load-transfer in piles, which is strongly associated with pile-soil interactions (Haigh and Madabhushi 2011). Hence, a proper model for pile-soil interactions is required to describe the behaviour of a pile.

To study the load-transfer mechanism in a pile, a simple linear model (Chow 1986) was first proposed for analytical analysis. This model can successfully describe the elastic behaviour of a pile. To simulate non-linear behaviour of a pile, the elastic-perfectly plastic model (Zhou 1991, Matyas and Santamarina 1994) was proposed, which assumed that the mobilized skin friction (or resistance) is constant even as the strain (or deformation) of the pile-soil interface increases in the plastic region. In other words, the influence of plastic deformation on skin friction is not considered in such a model. To account for the contribution of plastic deformation to the skin friction, a hybrid model (Zhu and Chang 2002) and a hyperbolic function model (Kim *et al*. 1999, Cao *et al*. 2014) were proposed. In these models, skin friction increases with plastic deformation at a pile-soil interface at a reduced rate, e.g., a hyperbolic relationship is used for this case. These models are only applicable in situations where the soil that surrounds a pile exhibits strain-hardening behaviour. However, over-consolidated clays or dense sands surrounding a pile may exhibit strain-softening behaviour, which has been reported by many researchers (Reese *et al*. 2006, Zou *et al*. 2010). In such situations, the bearing resistance of a pile might decrease with the plastic deformation of a pile-soil interface. As a result, the axial bearing capacity of the pile might be overestimated. Hence, greater attention has been given to the softening behaviour of the pile-soil interface. Liu *et al*. (2004) and Yao *et al*. (2012) used a tri-line model to describe the softening behaviour. In this model, the relationship between the skin friction of a pile and pile-soil relative displacement is simplified as a poly-line composed of three straight lines. However, a pile-soil interface generally exhibits a highly nonlinear behaviour. Hence, more advanced models should be used.

In this study, a softening model of the pile-soil interface is used to derive an analytical solution to investigate the load-transfer mechanism of a single pile under axial loading. Subsequently, a pile load test was performed to verify the newly developed analytical solution. Finally, a parametric analysis was performed to investigate the effects of the initial shear modulus and the ratio of the residual skin friction to the peak skin friction on the load-settlement curve of a pile.

2. Mechanism of the pile-soil interaction

2.1 Relationship between pile strain and pile-soil interface strain

To maintain displacement consistency at the pile-soil interface, it is assumed that

$$\omega_p(z) = \omega_i(z) \tag{1}$$

where $\omega_p(z)$ and $\omega_i(z)$ are the settlement of the pile and pile-soil interface at a depth z, respectively. The settlement of a pile consists of the settlement of the sub-soil layer under the pile, ω_{pb}, and the deformation of a pile segment below depth z, ω_{pd}

$$\omega_p(z) = \omega_{pb} + \omega_{pd}(z) \tag{2}$$

From Eqs. (1) and (2), we can obtain

$$\omega_{pb} + \omega_{pd}(z) = \omega_i(z) \tag{3}$$

In Eq. (3) ω_{pb} is independent of depth z, whereas both ω_{pd} (z) and ω_i (z) are a function of z. The shear strain of pile-soil interface is defined as

$$\varepsilon = \frac{d\omega_i(z)}{dz} \tag{4}$$

By differentiating Eq. (3), the relationship between the strain of pile (ε_p) and the shear strain at a pile-soil interface can be obtained

$$\varepsilon_p = \varepsilon \tag{5}$$

2.2 Relationship between the skin friction and shear strain at the pile-soil interface

A softening model that was proposed by Zheng *et al*. (2003), which was originally used to describe soil behaviour, was modified to simulate the softening behaviour at the pile-soil interface

$$\frac{\tau}{\tau_m} = \frac{\varepsilon(a + c\varepsilon)}{(a + b\varepsilon)^2} \tag{6}$$

where τ is the skin friction at the pile-soil interface; τ_m is the maximum skin friction; and a, b and c are parameters calibrated by experimental data. Fig. 1 schematically shows the stress-strain curve, where $1/a$ is the initial slope of the curve. The maximum stress ratio is $1/4(b - c)$, and hence, it is required that $1/4(b - c) = 1$. At the maximum stress ratio, the corresponding strain is $(-a)/(b - 0.5)$, beyond which the softening behaviour dominates. The residual stress ratio is c/b^2 when ε approaches infinity.

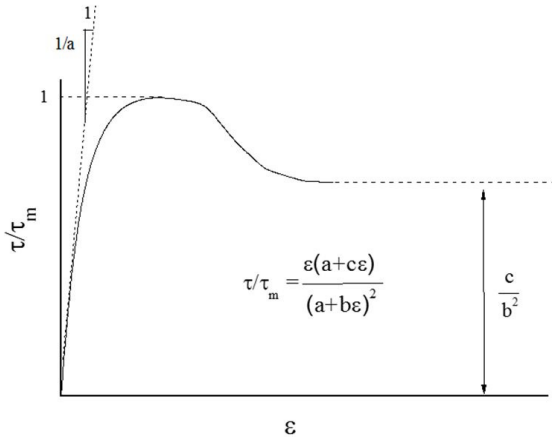

Fig. 1 Softening model of the pile-soil interface

It is assumed that the maximum shear stress τ_m can be determined from the following equation

$$\tau_m = \sigma_x \tan\varphi_i \tag{7}$$

where σ_x is the lateral earth pressure and φ_i is the friction angle of the pile-soil interface. This interface angle is affected by many factors, e.g., soil properties, pile properties and pile installation method. For simplicity, an empirical equation proposed by Randolph and Wroth (1980) is used

$$\varphi_i = \tan^{-1}\left(\frac{\sin(\varphi_s)\cos(\varphi_s)}{1+\sin^2(\varphi_s)}\right) \tag{8}$$

where φ_s is the friction angle of the soil. It is also assumed that the soil surrounding the pile is uniform and hence the lateral earth pressure is

$$\sigma_x = \gamma'_s z K_o \tag{9}$$

where γ'_s is the effective unit weight of the soil, and K_o is the coefficient of the earth pressure at rest. For normally consolidated soils, K_{on} is determined by Jaky (1948)

$$K_{on} = 1 - \sin\varphi_s \tag{10}$$

According to Mayne and Kulhawy (1982), the coefficient of earth pressure at rest for over-consolidated soils is

$$K_{oo} = K_{on}(OCR)^{\sin(\varphi_s)} \tag{11}$$

where OCR is the over-consolidation ratio. Combining Eqs. (10) and (11) yields the coefficient of earth pressure at rest for both normally consolidated and over-consolidated soils

$$K_o = (1-\sin\varphi_s)(OCR)^{\sin(\varphi_s)} \tag{12}$$

Substituting Eqs. (7), (9) and (12) into Eq. (6) yields

$$\tau = \gamma'_s \tan(\varphi_i)(1-\sin\varphi_s)(OCR)^{\sin(\varphi_s)}\frac{\varepsilon(a+c\varepsilon)}{(a+b\varepsilon)^2}z \tag{13}$$

2.3 Governing equation for single pile under axial loading

As shown in Fig. 2, the force equilibrium along the single pile yields

$$P_p(z) = C_p\tau_p(z)dz + P_p(z) + dP_p(z) \tag{14}$$

where $P_p(z)$ is the axial force of the pile at depth z; $\tau_p(z)$ is the skin friction of the pile at depth z; C_p is the circumference of the pile. For a circular pile, $C_p = 2\pi r_p$. Then, the above equation is written as

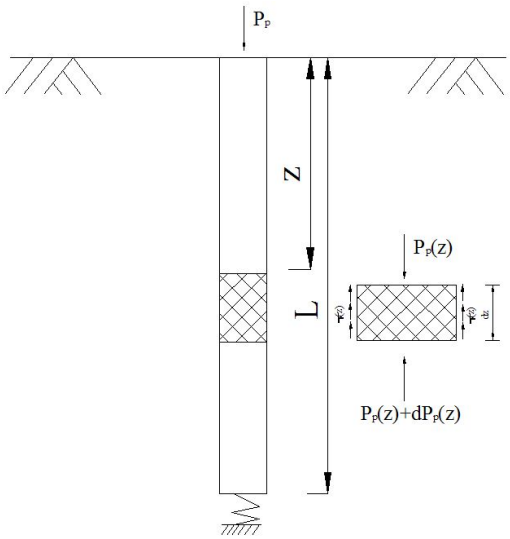

Fig. 2 Load-transfer model of a pile

$$\frac{dP_p(z)}{dz} = -2\pi r_p \tau_p(z) \tag{15}$$

Assuming the deformation of the pile is elastic, the relationship between the axial force and its strain is expressed as

$$\varepsilon_p = \frac{P_p(z)}{E_p A_p} \tag{16}$$

where E_p is elastic modulus of the pile and A_p is the cross-section area of the pile. For a circular pile, $A_p = \pi r_p^2$

Combining Eqs. (15) and (16) yields

$$\frac{d\varepsilon_p}{dz} = -\frac{2}{E_p r_p}\tau_p(z) \tag{17}$$

Substituting Eqs. (5) and (13) into the above equation yields

$$\frac{d\varepsilon_p}{dz} = -A\frac{\varepsilon_p(a+c\varepsilon_p)}{(a+b\varepsilon_p)^2}z \tag{18}$$

where $A = \dfrac{\gamma_s' \tan(\varphi_i)(1-\sin\varphi_s)(OCR)^{\sin(\varphi_s)}}{E_p r_p}$. Solving Eq. (18) gives the following results

$$\frac{\left[(ac^2 - 2abc + ab^2)\ln(c\varepsilon_p + a) - cb^2\varepsilon_p - ac^2\ln(\varepsilon_p)\right]}{c^2} - \frac{1}{2}Az^2 + M = 0 \tag{19}$$

where M is an integral constant, which can be obtained by the following boundary condition

$$\varepsilon_p\big|_{z=0} = \frac{P_p}{E_p \pi r_p^2} \tag{20}$$

The integral constant is obtained as follows

$$M = -\frac{\left[(ac^2 - 2abc + ab^2)\ln\left(c\frac{P_p}{E_p\pi r_p^2} + a\right) - cb^2\frac{P_p}{E_p\pi r_p^2} - ac^2\ln\left(\frac{P_p}{E_p\pi r_p^2}\right)\right]}{c^2} \tag{21}$$

Then, the relationship between the pile strain and depth is obtained

$$\begin{aligned} &\frac{(ac^2 - 2abc + ab^2)\ln\left(c\frac{P_p}{E_p\pi r_p^2} + a\right) - cb^2\frac{P_p}{E_p\pi r_p^2} - ac^2\ln\left(\frac{P_p}{E_p\pi r_p^2}\right)}{c^2} \\ &- \frac{(ac^2 - 2abc + ab^2)\ln(c\varepsilon_p + a) - cb^2\varepsilon_p - ac^2\ln(\varepsilon_p)}{c^2} - \frac{1}{2}Az^2 = 0 \end{aligned} \tag{22}$$

Combining Eqs. (13) and (22) yields the relationship between τ/τ_m and z. Settlement at the top of the pile, ω_{pt}, consists of the deformation of the entire pile ω_{pd} and the settlement at the pile toe ω_{pb}

$$\omega_{pt} = \omega_{pd} + \omega_{pb} \tag{23}$$

where $\omega_{pd} = \int_0^L \varepsilon_p dz$ and L is the length of the pile. Based on the Boussinesq solution (Timoshenko and Goodier 1951), ω_{pb} is calculated as follows

$$\omega_{pb} = n_b P_b \tag{24}$$

where P_b is the load at the pile toe; and $n_b = \eta(1 - v_b) / 4r_p G_b$ and η are empirical parameters of the pile toe displacement. η is generally a value within 0.5 to 1 (Xiao *et al*. 2003), and hence, a value of 0.75 was chosen in this study. v_b and G_b are Poisson's ratio and the shear modulus of the soil at the pile toe, respectively.

3. Verification of the proposed model

3.1 Field pile load test

A field pile load test on a single pile was conducted to verify the derived analytical solution. Fig. 3 shows its schematic diagram and a photograph of the set-up for the pile load test. The loads were applied on a loading frame attached to the pile by using a hydraulic jack against a reaction

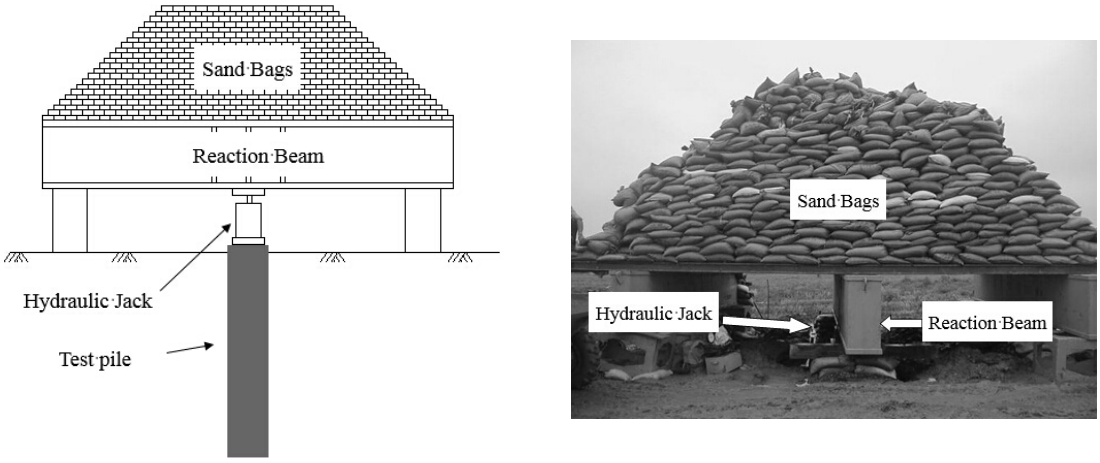

(a) Schematic diagram (b) Photograph

Fig. 3 Set-up for the pile load test

beam.

In the field test, the surface ground was relatively flat, and no surcharge was applied. The ground water table was located near ground surface. The pile consisted of C30 concrete, where the compressive strength of the concrete was 30 MPa. The length of pile was 45 m with a diameter of 1.5 m. First, the pile was driven to the desired depth. Then, loads were applied incrementally from 1,500 kN to 16,000 kN. The quick-maintained-load method was used for the field test. A load increment of 1,500 kN was applied approximately every 2.5 min. Subsurface soil exploration was performed near the test pile, and hence, the geotechnical properties of the soils surrounding the pile were obtained. The soil strata were relatively uniform and consisted of a clay layer that exhibited a relatively high density and a high plasticity.

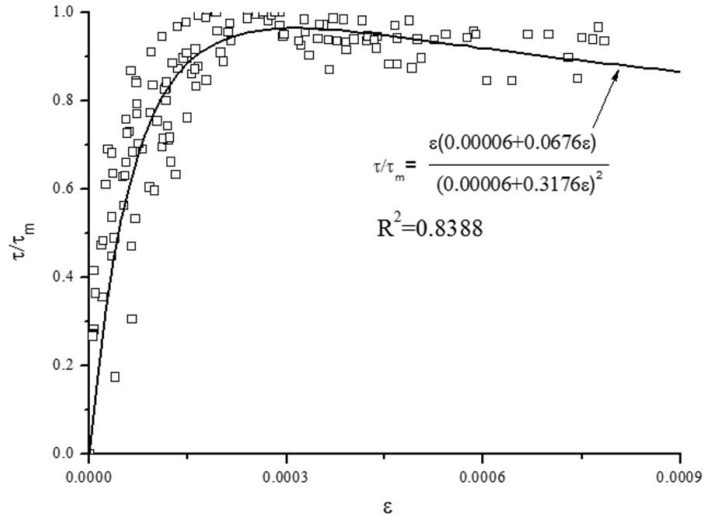

Fig. 4 Calibration of the softening model of the pile-soil interface

Table 1 Parameters for the analytical solution

Pile-soil interaction			Surrounding soil			Pile-toe soil		Pile		
a	b	c	γ'_s	φ_s	OCR	E_s	v	L	r_p	E_p
0.00006	0.3176	0.0676	8 kN/m^3	20°	1.5	24 MPa	0.3	45 m	0.75 m	10 GPa

Load cells and strain gauges were installed along the pile at 7 depths (5.0 m, 12.8 m, 18.8 m, 24.8 m, 31.0 m, 36.0 m, 41.0 m). At each depth, four load cells and four strain gauges were used to measure the axial force and strain of the pile. At the pile toe, two load cells were installed to measure the toe resistance of the pile. Based on the measurement of the axial force along the pile, the skin friction was calculated using Eq. (15).

3.2 Calibration of the softening model for the pile-soil interface

Fig. 4 shows the measured shear strain of the pile and skin friction for the pile-soil interface. Based on these field test results, Eq. (6) was calibrated. Using the least squares integral method, a, b and c were determined to be 0.00006, 0.3176 and 0.0676, respectively. It should be noted that the reduction after the peak value can be described by the softening model. Other parameters used in the analytical solution are summarised in Table 1.

3.3 Axial force of the pile

Fig. 5 shows the comparison between the axial forces of the pile obtained from the measured and analytical results. Five step loads from 1,500 kN to 16,000 kN were chosen to verify the softening model. Good agreement was obtained for the softening model under these five loads. The axial force equals the applied load when the depth is zero. The axial force decreases as the depth increases. Within a depth of 7 m, the axial force only slightly changes, possibly due to the small lateral earth pressure acting on the pile. When the depth is greater than 7 m, the axial force

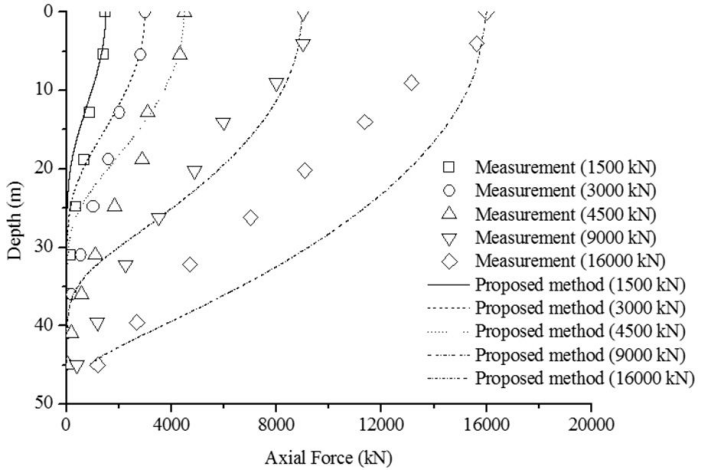

Fig. 5 Axial force profiles at different applied loads

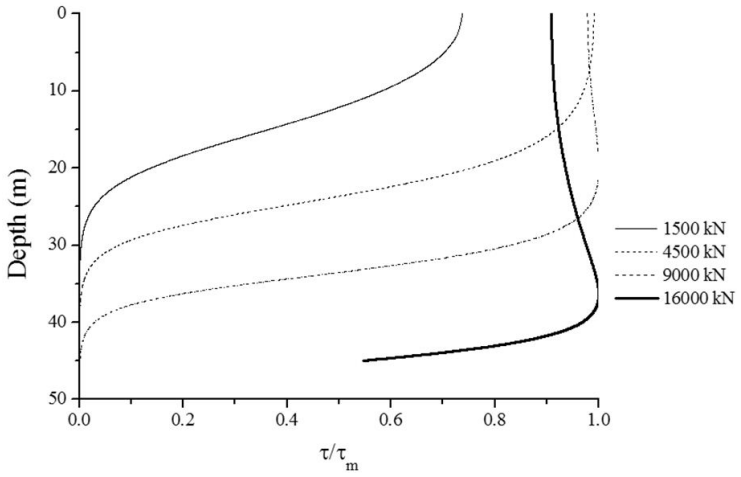

Fig. 6 Normalized skin friction profiles at different applied loads

rapidly decreases, which suggests that skin friction works effectively. For different applied loads, the axial force profiles exhibit a similar trend.

3.4 Normalised skin friction profile

Fig. 6 shows the normalised skin friction (τ/τ_m) profiles for different applied loads. When the load is small (i.e., 1,500 kN), τ/τ_m is approximately 0.7 at the top of the pile and then decreases to zero at a depth of 30 m. When the load increases to 4,500 kN, a similar change in τ/τ_m with depth is observed. The depth at which τ/τ_m equals zero increases with the applied load. When the load is 9,000 kN, τ/τ_m within a depth of 25 m is almost 1.0, which indicates that the skin friction is fully mobilised, i.e., reaches its peak skin friction. At the pile toe, τ/τ_m is still zero, which indicates that the toe bearing is not yet mobilised. When the load is 16,000 kN, τ/τ_m within a depth of 25 m decreases to approximately 0.9, which indicates that the pile-soil interface softens. This behaviour is generally ignored by most existing analytical solutions. τ/τ_m within a depth from 25 to 40 m reaches 1.0, at which the peak skin friction is mobilised. At the pile toe, τ/τ_m increases to 0.53, which indicates that the toe resistance begins to play an important role in the pile resistance.

4. Parametric analysis

4.1 Effect of the initial shear modulus

As showed in Fig. 1, the initial slope of the shear strain-stress curve or the initial shear modulus of the pile-soil interface is determined by the value of parameter a. Fig. 7 shows the total skin friction- and load-settlement curves obtained from the newly developed analytical solution using different values of a (i.e., 0.00006, 0.00012, 0.00018 and 0.00024) with $c / b^2 = 0.69$. At the beginning, the settlement at the pile top almost linearly increases with the applied load until the load reaches a threshold value, P_t. The P_t is defined as the load where the total skin friction begins to deviate from the applied load. Below P_t, the total friction is equal to the applied load, which

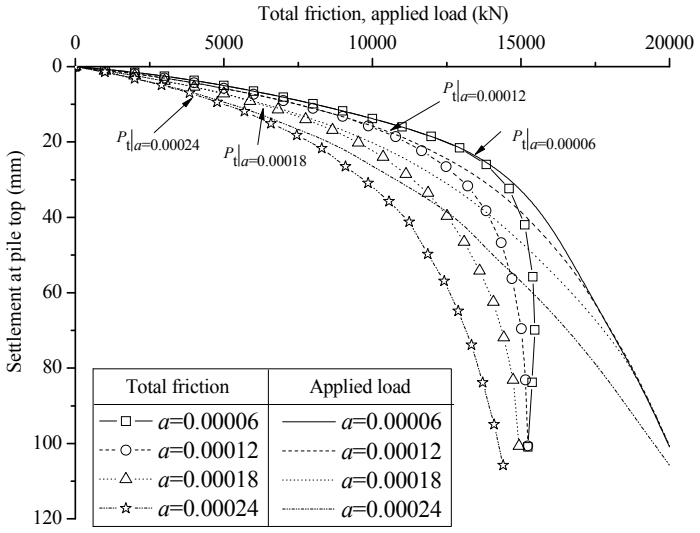

Fig. 7 Effect of the initial shear modulus on the total skin friction- and load-settlement curves with $c / b^2 = 0.69$

suggests that the initial pile resistance is mainly attributed to the skin friction. As expected, the higher the value of a, the lower the initial shear modulus and thus the larger the slope of load-settlement curve. However, P_t decreases with an increased value of a. When a equals 0.00006, P_t is approximately 14,000 kN. When a reaches 0.00024, P_t decreases to 3,700 kN, only approximately 26% of the case with a = 0.00006. Beyond P_t, the settlement increases at an accelerated rate; however, the rate decreases with the value of a, exhibiting an opposite behaviour with the case below P_t. The total skin friction-settlement curves tend to converge into a vertical asymptotic line. This observation is because the curves have the same value of c / b^2, which controls the residual skin friction and hence the ultimate total skin resistance. In other words, the value of a primarily controls the curvature of the total skin friction- and load-settlement curves. It should be noted that only the total skin friction-settlement curve with a = 0.00006 shows slightly softening behaviour. It may be due to a relatively high value of c / b^2.

4.2 Effect of the ratio of residual to peak skin frictions

As shown in Fig. 1, the residual stress ratio is c / b^2, where its value indicates the degree of softening. A lower value of c / b^2 indicates a stronger softening behaviour. Five values of c / b^2 (i.e., 0.2, 0.4, 0.6, 0.8, 1.0) were used to compute the total skin friction- and load-settlement curves (with a = 0.00006), and the results are shown in Fig. 8. It should be noted that when c / b^2 = 1.0 (i.e., residual skin friction equals the peak skin friction), the model retrogresses into a hardening model. Similar to Fig. 7, the curves in Fig. 8 illustrate that the settlement increases with load initially at an almost constant rate until P_t is reached and then the increasing rate rises up dramatically. The initial segment of the five load-settlement curves appears to be independent of the ratio of the residual to peak skin frictions. Moreover, the value of P_t seems not to be affected by c / b^2. As the value of c / b^2 decreases, the total skin friction-settlement curve shows more obvious softening behaviour, i.e., total skin friction may decrease with further increase in

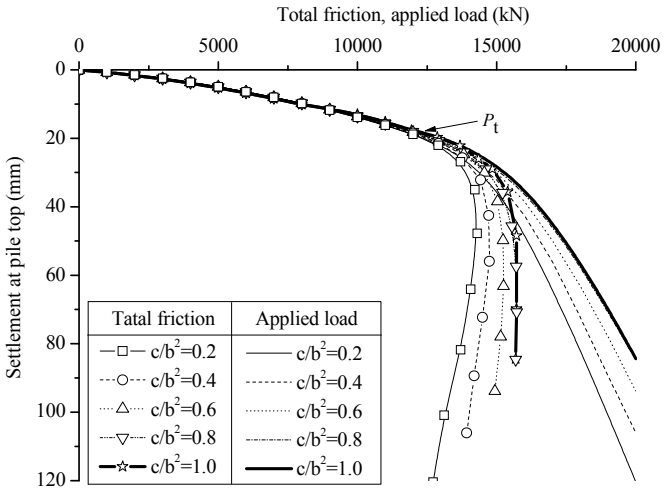

Fig. 8 Effect of the ratio of the residual skin friction to peak skin friction on total skin friction- and load-settlement curves with a = 0.00006

settlement at pile top. If the allowable settlement is set at 3% of the pile diameter (i.e., 45 mm) (Muni 2001), the allowable load capacity with c/b^2 = 0.2 is 15,652 kN and the corresponding total skin friction is 14,203 kN. As c/b^2 increases to 1.0, the allowable load capacity is 17,104 kN and the corresponding total skin friction is 15,667 kN. Thereby, the decrease in load capacity is 1,452 kN as c/b^2 decreases from 1.0 to 0.2, which is very close to that in total friction (i.e., 1,464 kN). This comparison indicates that although the same peak skin friction is used, the load capacity of the pile is reduced by 8.5% as c/b^2 decreases from 1.0 to 0.2.The decrease of load capacity is mainly attributed to the loss of total skin friction, clearly reflecting the softening behaviour of the pile-soil interface. Therefore, the softening behaviour of the pile-soil interface cannot be ignored during design; otherwise, the pile load capacity will be over-estimated.

5. Conclusions

A nonlinear softening model of the pile-soil interface is used to derive an analytical solution for a single pile under axial loading. Hence, the analytical solution was verified by the results from a field pile load test, and a parametric analysis was further conducted. The following conclusions can be drawn from this study:

- The analytical solution was verified by its good agreement between the analytical solution and test results regarding the pile axial force and stress-strain relationship of the pile-soil interface. The softening behaviour of the skin friction could be simulated well when the pile is subjected to large loads.
- The value of a primarily controls the initial segment of the load-settlement curves and P_t, whereas the ultimate load is determined by the value of c/b^2. P_t is the threshold value of the load at which the friction begins to be inconsistent with the applied load. Below P_t the applied load at the top only transfers into the skin friction, otherwise into the skin friction and toe resistance.

- If softening behaviour of the pile-soil interface is ignored, the axial load capacity of a single pile will be over-estimated.

Acknowledgments

The authors would like to acknowledge financial supports from a research grant (No. 51279049) provided by the National Natural Science Foundation of China, a fundamental research funds (No. 2014B04914) for the Central Universities, a research grant (No. 2013CB036404) provided by the Ministry of Science and Technology in China under the National Basic Research Program (the 973 Program) and a research grants (No. 51308164) provided by the National Natural Science Foundation of China.

References

Cao, W., Chen, Y. and Wolfe, W.E. (2014), "New load transfer hyperbolic model for soil-pile interface and negative skin friction on single piles embedded in soft soils", *Int. J. Geomech.*, *ASCE*, **14**(1), 92-100.

Chow, Y.K. (1986), "Analysis of vertically loaded pile groups", *Int. J. Numer. Anal. Methods Geomech.*, **10**(1), 59-72.

Haigh, S.K. and Madabhushi, S.P.G. (2011), "Centrifuge modelling of pile-soil interaction in liquefiable slopes", *Geomech. Eng*, *Int. J.*, **3**(1), 45-59.

Jaky, J. (1948), *Pressure in Soils*, (2nd ICSMFE), London, UK, Volume 1, pp. 103-107.

Kim, S., Jeong, S., Cho, S. and Park, I. (1999), "Shear load transfer characteristics of drilled shafts in weathered rocks", *J. Geotech. Geoenviron. Eng.*, **125**(11), 999-1010.

Liu, J., Xiao, H.B. Tang, J. and Li, Q.S. (2004), "Analysis of load-transfer of single pile in layered soil", *Comput. Geotech.*, **31**(2), 127-135.

Madhav, M.R., Sharma, J.K. and Sivakumar, V. (2009), "Settlement of and load distribution in a granular piled raft", *Geomech. Eng*, *Int. J.*, **1**(1), 97-112.

Matyas, E. and Santamarina, J.C. (1994), "Negative skin friction and the neutral plane", *Can. Geotech. J.*, **31**(4), 591-597.

Mayne, P.W. and Harris, D.E. (1993), "Axial load-displacement behavior of drilled shaft foundations in piedmont residuum", FHWA no. 41-30-2175; Georgia Tech Research Corporation, Geotechnical Engineering Division, Georgia Institute of Technology, School of Civil Engineering, Atlanta, GA, USA.

Mayne, P.W. and Kulhawy, F.H. (1982), "K0-OCR relationships in soil", *J. Geotech. Eng.*, **108**(GT6), 851-872.

Muni, B. (2001), *Soil Mechanics and Foundations*, John Wiley & Sons, Inc.

Poulos, H.G. (1988), "Pile-behavior-theory and application", *Geotechnique*, **39**(3), 365-415.

Reese, L.C., Isenhower, W.M. and Wang, S. (2006), *Analysis and Design of Shallow and Deep Foundations*, John Wiley & Sons, Inc.

Randolph, M.F. and Wroth, C.P. (1980), "Application of the failure state in undrained simple shear to the shaft capacity of driven piles", *Geotechnique*, **31**(1), 143-157.

Timoshenko, S.P. and Goodier, J.N. (1951), *Theory of Elasticity*, McGraw- Hill.

Vesic, A.S. (1961), "Bending of beams resting on isotropic elastic solids", *J. Eng. Mech. Div.*, *ASCE*, **87**(EN2), 35-63.

Xiao, H.B., Zhong, H.H. and Wan, Y.H. (2003), "Analysis of pile's load transfer in layered soils", *J. Central South Univ. Technol.*, **34**(6), 687-690.

Yao, W.J., Liu, Y.M. and Chen, J. (2012), "Characteristics of negative skin friction for super-long piles under surcharge loading", *Int. J. Geomech.*, **12**(2), 90-97.

Zheng, Y.R., Shen, Z.J. and Gong, X.N. (2003), *The Principles of Geotechnical Plastic Mechanics*, Chinese

Architecture and Building Press, Beijing, China.
Zhou, G.L. (1991), "An analysis on the mechanism of negative skin friction for single piles", *Rock Soil Mech*., **12**(3), 35-42.
Zhu, H. and Chang, M.F. (2002), "Load transfer curves along bored piles considering modulus degradation", *J. Geotech. Geoenviron. Eng*., **128**(9), 764-774.
Zou, J., Zhang, Z., Liu, J. and He, J. (2010) "A load transfer model considering strain softening of soils", *Chinese J. Geotech. Eng*., **32**(7) 1109-1113.

CC